J Mater Sci: Mater Electron **(2025) 36:600**

Potential of Be_2FeX (X = Ag, Au, Cd, Cu, Ga, Zn) Heusler alloys for spintronics and energy conversion technologies

Erol Albayrak[1,*]

[1] *Department of Metallurgy and Materials Engineering, Kirsehir Ahi Evran University, 40100 Kırsehir, Turkey*

Received: 12 January 2025
Accepted: 24 March 2025
Published online: 4 April 2025

ABSTRACT

The aim of this study is to investigate the structural, electronic, magnetic, elastic and thermodynamic properties of Be_2FeX (X = Ag, Au, Cd, Cu, Ga, Zn) Heusler alloys. These alloys, which contain the elements Be and Fe, have important applications, particularly in the aerospace industry, although they have attracted attention due to their toxic nature. Calculations using Quantum Espresso and Thermo Pw packages based on the DFT approach showed that all alloys are mechanically stable according to born stability criteria. The Be_2FeAg alloy, with its moderate hardness and ductility, is suitable for structural applications where high hardness and ductility are not required. The metallic conductivity of the alloy suggests potential applications in areas such as spintronic devices, energy conversion and storage devices. Be_2FeAu alloy is suitable for applications requiring mechanical strength with low ductility and medium hardness (Young's modulus value of 161.93 GPa). Be_2FeCd alloy offers significant potential for magnetic data storage and sensing applications due to its high ductility and metallic conductivity (B/G rate of 2.35). Be_2FeCu alloy, with its high hardness (Young's modulus value of 241.862 GPa) and low ductility, is ideal for applications where mechanical strength is critical. Be_2FeGa alloy, with its flexible structure (B/G rate of 3.55), is suitable for energy efficiency and optoelectronic devices. Be_2FeZn alloy, with its medium hardness (Young's modulus value of 164.29GPa) and ductility (B/G rate of 2.16), has the potential for use in high temperature applications. Understanding the properties of these alloys can provide guidance for future technological applications and new materials development processes.

1 Introduction

Following their discovery in 1903, Heusler alloys have become a significant research area within the field of modern materials science. These intermetallic compounds are categorized as full and semi-Heusler alloys, with the respective chemical formulae X_2YZ and XYZ [1–6]. The properties of these alloys, which include magnetic, electronic, structural, thermal stability and heat capacity, have led to their extensive utilization in numerous technological applications. Notably, their wide band gaps and high charge transport

Address correspondence to E-mail: erol.albayrak@ahievran.edu.tr

https://doi.org/10.1007/s10854-025-14666-6

mobility have rendered them prominent materials in energy applications [7].

The ferromagnetic and antiferromagnetic phase transitions of Heusler alloys have made them important for spintronic applications, and the topological properties of some Heusler alloys have also contributed to the development of advanced quantum materials [8]. Recent high-resolution spectroscopic analyses and advanced computational methods have provided significant insights into the synthesis and structural, electronic, elastic, thermal and vibrational properties of these alloys [9–15]. It has also been demonstrated that the electronic and magnetic properties of Heusler alloys can be tuned by controlling some properties at the atomic level.

Density Functional Theory (DFT) is a widely used computational method to study the electronic and magnetic structures of Heusler alloys [16]. DFT enables comprehension of the fundamental properties of materials based on the principles of quantum mechanics, facilitating detailed study of material interactions and band structures. In 2022, Huang and colleagues demonstrated that point defects can be engineered to enhance the thermoelectric performance of Heusler alloys [12]. These computational studies provide valuable guidelines for experimental research.

The physical and chemical properties of Heusler alloys are such that they are considered ideal material candidates for modern technology; this study investigates the possible application areas of Be_2FeX (X = Ag, Au, Cd, Cu, Ga, Zn) Heusler alloys and the technological potential of these alloys. In addition, the study investigates how the properties of these alloys can be optimized by advanced computational methods. The studies carried out in this context will guide future experimental investigations.

2 Method

The aim of this study is to understand the structural, electronic, elastic and thermal properties of Be_2FeX (X = Ag, Au, Cd, Cu, Ga, Zn) Heusler alloys and to predict their possible applications in technology. For this purpose, the Quantum Espresso (QE) package program based on the density functional theory (DFT) approach was used. QE is an open-source package program used for plane wave-based DFT calculations with a wide range of applications in materials science [17–19]. To determine the stable states of molecules in the calculations, it is necessary to calculate the minimum energy state of the molecule. To calculate the minimum energy, the electronic ground-state charge density and exchange correlation potential of the material must be determined. The Perdew–Burke–Ernzehof generalized gradient approximation (PBE-GGA) was used to determine the exchange correlation potential [20]. The pseudo potentials used for the effects on the wave function due to the interaction of the cor and valence electrons of atoms were chosen from the Rappe group. The kinetic energy cutoff for the wave functions was chosen as 40 Ry, and the electronic charge density cutoff was 400 Ry. For calculations in the vicinity of the Fermi surface, the Smearing Smearing parameter was chosen as 0.05 Ry. The Thermo Pw (TP) program was used to calculate the thermodynamic properties and elastic constants of the alloy. It was assumed that pressure was applied to the alloy, and elastic constants were calculated from the energy difference between the distorted and undistorted crystal structures of the alloy under this pressure [21, 22]. After the elastic constants were calculated, the moduli, which help us understand some of the properties of the alloys, such as ductility and hardness, were calculated via these elastic constants. Thermodynamic calculations of the alloy were based on the Debye model.

3 Results and discussion

3.1 Structural properties

Representative unit cell structures of Be_2FeX (X = Ag, Au, Cd, Cu, Ga, Zn) Heusler alloys whose atoms are arranged according to the Fm-3 m space group and crystallize in the $L2_1$ phase are shown in Fig. 1.

The positions of the atoms of the Be_2FeX (X = Ag, Au, Cd, Cu, Ga, Zn) Heusler alloys in the unit cell are given in Table 1, including the (x, y, z) coordinates.

The calculated steady-state optimized lattice constants for the minimum energy values of the alloys, the moduli obtained via these constants and several constants are given in Table 2.

The elastic constants play a very important role in all the given equations. After calculating these constants, the aforementioned modulus and ratios were calculated using the equations [23–26]. As a result of the calculations, we found that Be_2FeX (X = Ag, Au, Cd, Cu, Ga, Zn) alloys meet the Born stability criteria. Born stability criteria that allow us to understand that

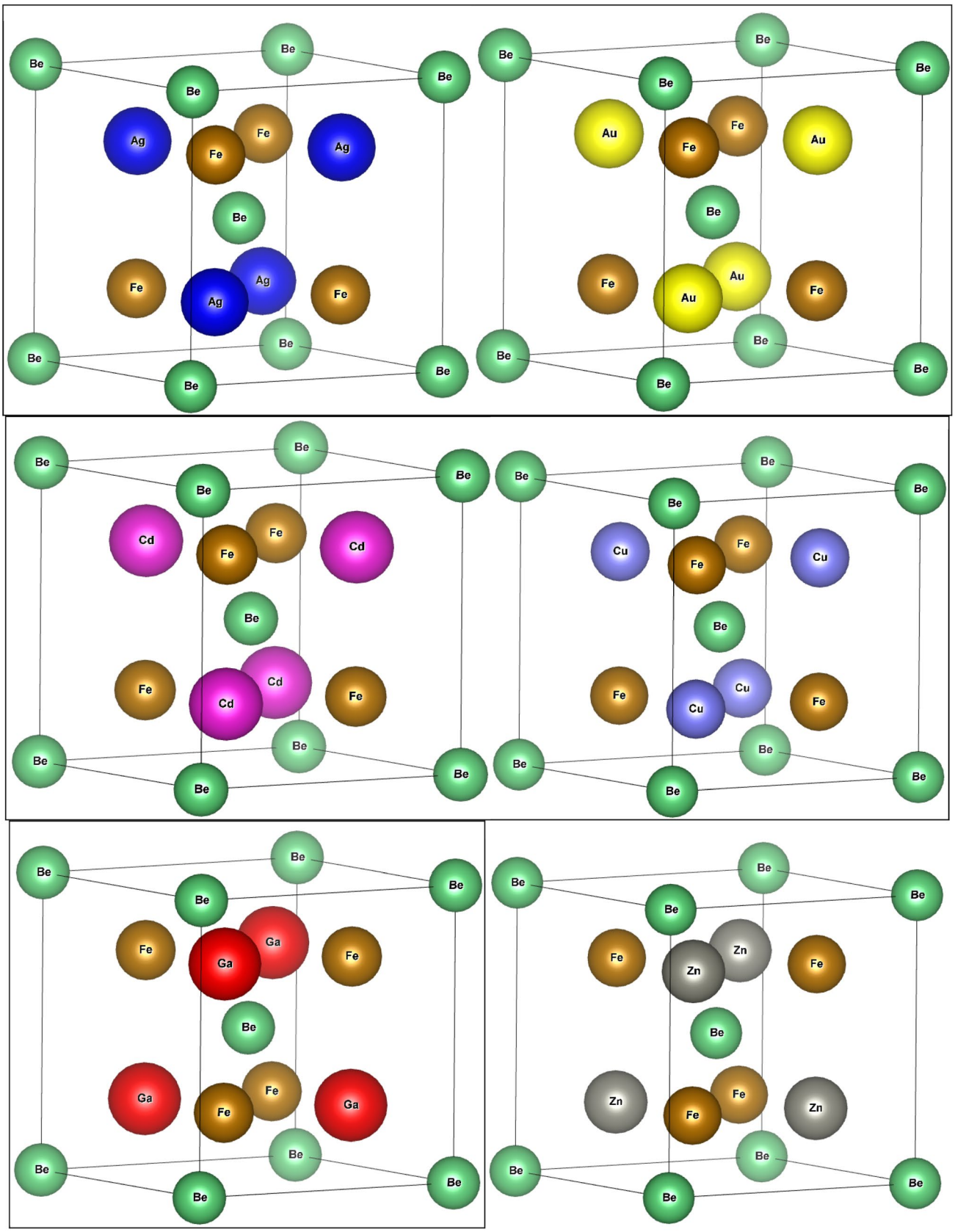

Fig. 1 Representative unit cell structures of Be_2FeX (X = Ag, Au, Cd, Cu, Ga, Zn) Heusler alloys in the Fm-3 m space group

Table 1 Positions (x, y, z) of the Be_2FeX (X = Ag, Au, Cd, Cu, Ga, Zn) Heusler alloys within the unit cell

Material	Position (Be (x, y, z))	Position (Fe(x, y, z))	Position (Ag, Au, Cd, Cu, Ga, Zn(x, y, z))
Be_2FeAg	(0, 0, 0)–(0.5, 0.5, 0.5)	(0.75, 0.75, 0.75)	(0.25, 0.25, 0.25)
Be_2FeAu	0, 0, 0)–(0.5, 0.5, 0.5)	(0.75, 0.75, 0.75)	(0.25, 0.25, 0.25)
Be_2FeCd	0, 0, 0)–(0.5, 0.5, 0.5)	(0.75, 0.75, 0.75)	(0.25, 0.25, 0.25)
Be_2FeCu	0, 0, 0)–(0.5, 0.5, 0.5)	(0.75, 0.75, 0.75)	(0.25, 0.25, 0.25)
Be_2FeGa	0, 0, 0)–(0.5, 0.5, 0.5)	(0.25, 0.25, 0.25)	(0.75, 0.75, 0.75)
Be_2FeZn	0, 0, 0)–(0.5, 0.5, 0.5)	(0.25, 0.25, 0.25)	(0.75, 0.75, 0.75)

Table 2 Calculated lattice parameters (a_o, Å), bulk modulus (B, GPa), shear modulus (G, GPa), Young's modulus (E, GPa), B/G ratio, Poisson's ratio (σ), anisotropy factor (A), and elastic constants (C_{11}, C_{12}, C_{44}, GPa) of Be_2FeX (X = Ag, Au, Cd, Cu, Ga, Zn) Heusler alloys

Materials	a_o	B	G	E	B/G	σ	A	C_{11}	C_{12}	C_{44}
Be_2FeAg	5.456	116.97	60.40	154.57	1.94	0.2796	1.71	175.34	87.79	74.93
Be_2FeAu	5.485	127.47	62.85	161.93	2.03	0.2881	1.60	190.75	95.83	75.86
Be_2FeCd	5.620	111.73	47.63	125.10	2.35	0.3132	1.66	158.57	88.32	58.40
Be_2FeCu	5.181	258.40	83.64	241.862	3.09	0.3433	2.18	333.75	220.72	123.00
Be_2FeGa	5.335	130.65	36.80	96.23	3.55	0.3073	34.45	135.41	128.27	106.15
Be_2FeZn	5.347	137.29	63.45	164.29	2.16	0.2947	3.59	176.45	117.70	105.56

the alloys are mechanically stable are given in Eq. (1). The bulk modulus was calculated via Eq. (2), shear modulus via Eq. (3), Young's modulus via Eq. (4), Poisson's ratio via Eq. (5), and the Anisotropy factor via Eq. (6) [27].

$$C_{44} > 0; C_{11} - C_{12} > 0; C_{11} + 2C_{12} > 0 \quad (1)$$

$$B = (C_{11} + 2C_{12})/3 \quad (2)$$

$$G = 5(C_{11} - 2C_{12}).C_{44}/3(C_{11} - 2C_{12}) + C_{44} \quad (3)$$

$$E = 9BG/3B + G \quad (4)$$

$$\sigma = \frac{1}{2}\left(1 - \frac{E}{3B}\right) \quad (5)$$

$$A = 2.C_{44}/(C_{11} - C_{12}) \quad (6)$$

The calculated bulk modulus of the alloys revealed that the Be_2FeCu alloy has the largest B value and that Be_2FeCd has the smallest B value. *The B* values of all the alloys are greater than 100 GPa, which means that all the alloys have low compressibility. Among them, the least compressible alloy was Be_2FeCu, and the least compressible alloy was Be_2FeCd. The Young's modulus can be used as a measure of hardness [22]. Hardness comparison can be made by examining the E values of the alloys. Considering this information, the hardest alloy was Be_2FeCu, and the softest alloy was Be_2FeGa. *The B/G* ratios of the alloys allow us to estimate their ductility. Since the B/G ratios of all the alloys are greater than 1.75, all the alloys are ductile. When the alloys were ranked among themselves, Be_2FeGa was the most ductile, and Be_2FeAg was the most brittle. Poisson's ratio of the alloys provides information about the characteristics of the atomic bonding in the alloys. Considering Poisson's ratio, the atomic bonds in all the alloys are predominantly ionic in character. In addition, the anisotropy factor of all the alloys is different from 1, and all the alloys are anisotropic.

4 Thermodynamic properties

The Debye temperature is a pivotal parameter in determining the elastic properties, atomic vibrations and low-temperature heat capacity of a material. It plays a significant role in understanding the physical behavior of solids at low temperatures and

Table 3 Debye temperatures calculated for Be_2FeX (X = Ag, Au, Cd, Cu, Ga, Zn) Heusler alloys (θ_{Debye}(K))

Material	Be_2FeAg	Be_2FeAu	Be_2FeCd	Be_2FeCu	Be_2FeGa	Be_2FeZn
θ_{Debye}	438.56	368.32	392.44	602.74	312.91	497.79

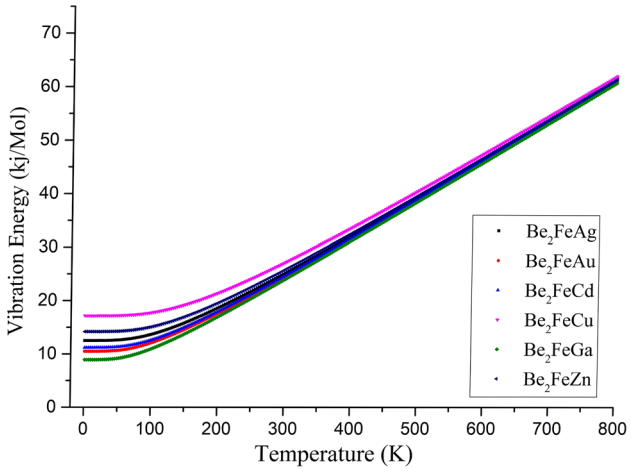

Fig. 2 Vibrational energy—temperature curves of Be_2FeX (X = Ag, Au, Cd, Cu, Ga, Zn) Heusler alloys

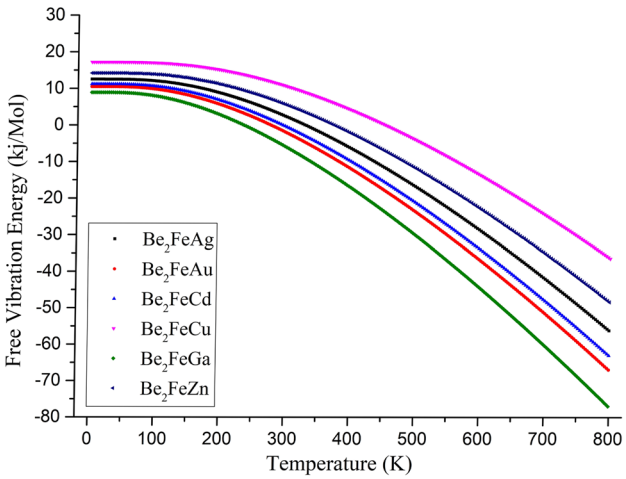

Fig. 3 Free vibrational energy—temperature curves of Be_2FeX (X = Ag, Au, Cd, Cu, Ga, Zn) Heusler alloys

is frequently evaluated in engineering fields such as thermal conductivity. The Thermo Pw program with the Debye model was used to understand the thermodynamic properties of the alloys. The calculated Debye temperatures for the alloys are given in Table 3.

A low Debye temperature indicates that the melting temperature of the material is low. This information means that materials with lower melting temperatures are more stable. Table 3 shows that the alloy with the lowest Debye temperature is Be_2FeGa, and on the basis of this information, this alloy is more stable than the others. The temperature-dependent changes in energy, free energy, entropy and heat capacities plotted in the Thermo Pw program for the alloys are given in Figs. 2, 3, 4 and 5.

Figure 2 shows that the vibration energy of the Be_2FeCu alloy is greater than that of the other alloys. The reason for this is that the mass of the Cu added to the Be_2Fe skeleton structure is smaller than the masses of the other elements added to the same skeleton structure. In accordance with the conservation of total energy, materials with high vibration energy are expected to have low free vibration energies. Figure 3 shows that the graph obtained was in accordance with expectations. When the entropy of the alloys is examined in Fig. 4, the Be_2FeCu alloy is the most regular, and the Be_2FeGa alloy is the most

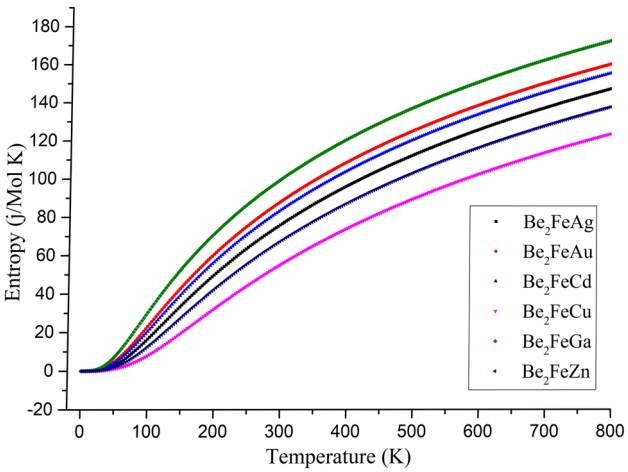

Fig. 4 Entropy—temperature curves of Be_2FeX (X = Ag, Au, Cd, Cu, Ga, Zn) Heusler alloys

irregular alloy. Finally, according to the heat capacity graphs of the alloys, the Be_2FeGa alloy has the highest heat capacity value, and the Be_2FeCu alloy has the lowest heat capacity value. Figure 5 shows that the heat capacity values of all three alloys are constant after approximately 300 K. This limit

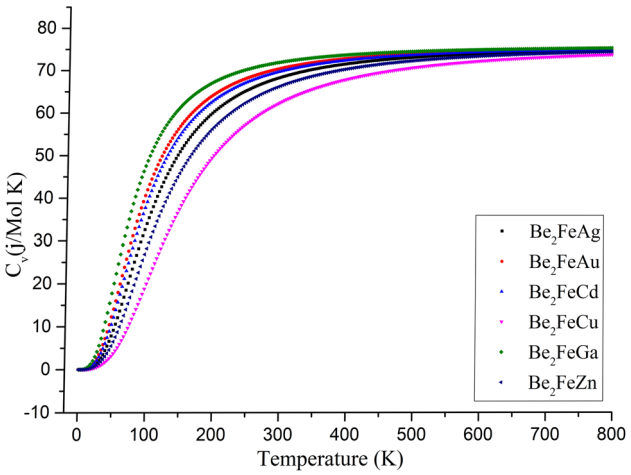

Fig. 5 Heat capacity—temperature curves of Be_2FeX (X = Ag, Au, Cd, Cu, Ga, Zn) Heusler alloys

reached by the heat capacity of the alloys is known as the Dulong-Petit limit [28].

5 Electronic properties

Electronic band graphs of the Be_2FeX (X = Ag, Au, Cd, Cu, Ga, Zn) alloys are shown in Fig. 6.

The electronic band graph of the Be_2FeAg alloy revealed that the curves belonging to the conduction and valence bands cut the Fermi energy level at the spin-up and spin-down axes. This helps us understand that there is no forbidden energy gap between the conduction and valence bands of the alloy. The fact that electrons can easily pass between the bands indicates that the Be_2FeAg alloy has a metallic conductive character. In addition, when the DOS graphs in Fig. 7 are examined, it is understood that this alloy has metallic properties. In light of this information, the Be_2FeAu alloy is metallic, the Be_2FeCd alloy is metallic, the Be_2FeCu alloy is metallic, the Be_2FeGa alloy is half metallic-like, and the Be_2FeZn alloy is metallic. A small gap between the curves on the spin-down symmetry axis of the Be_2FeGa alloy and the Fermi energy level indicates that this alloy may exhibit half metallic-like behavior. When Fig. 7 is examined, it is understood from which orbitals the electrons that contribute significantly to the conductivity of the alloys come from.

The calculated total magnetic moment values of the alloys are shown in Table 4.

According to the calculated values, the Be_2FeCd alloy has the highest magnetic moment, and the Be_2FeCu alloy has the lowest magnetic moment.

6 Conclusions

This study investigated the structural, electronic, magnetic, elastic, and thermodynamic properties of Be_2FeX (X = Ag, Au, Cd, Cu, Ga, Zn) Heusler alloys using DFT-based calculations. All alloys were found to be mechanically stable according to the Born stability criteria.

The Be_2FeAg alloy exhibits moderate hardness and ductility, making it suitable for structural applications and spintronic devices. Be_2FeAu, with low ductility and moderate hardness, is impact-resistant and suitable for energy storage and conversion applications. Be_2FeCd, possessing high ductility and strong ferromagnetism, shows promise for magnetic data storage and sensor applications. Be_2FeCu is the hardest alloy with excellent conductivity and high thermal stability, making it ideal for high-temperature electronic and mechanical applications. Be_2FeGa is highly ductile and exhibits half-metallic-like conductivity, making it suitable for flexible and optoelectronic devices. Be_2FeZn, with medium hardness and ductility, has potential in magnetic sensors, memory applications, and high-temperature environments.

These findings provide insights into the technological applications of these alloys and guide future experimental studies.

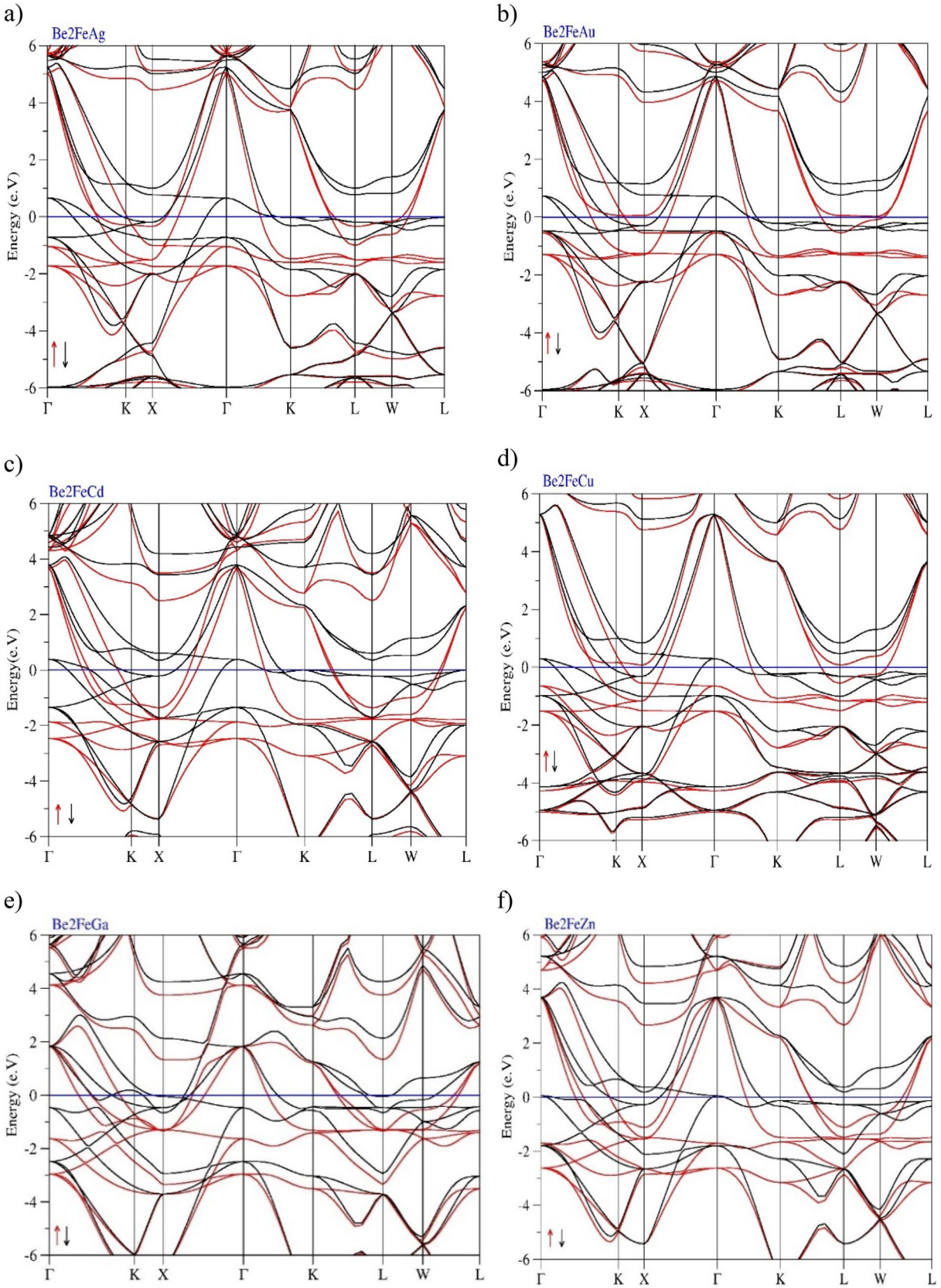

Fig. 6 Electronic band plots of Be_2FeX (X = Ag, Au, Cd, Cu, Ga, Zn) alloys

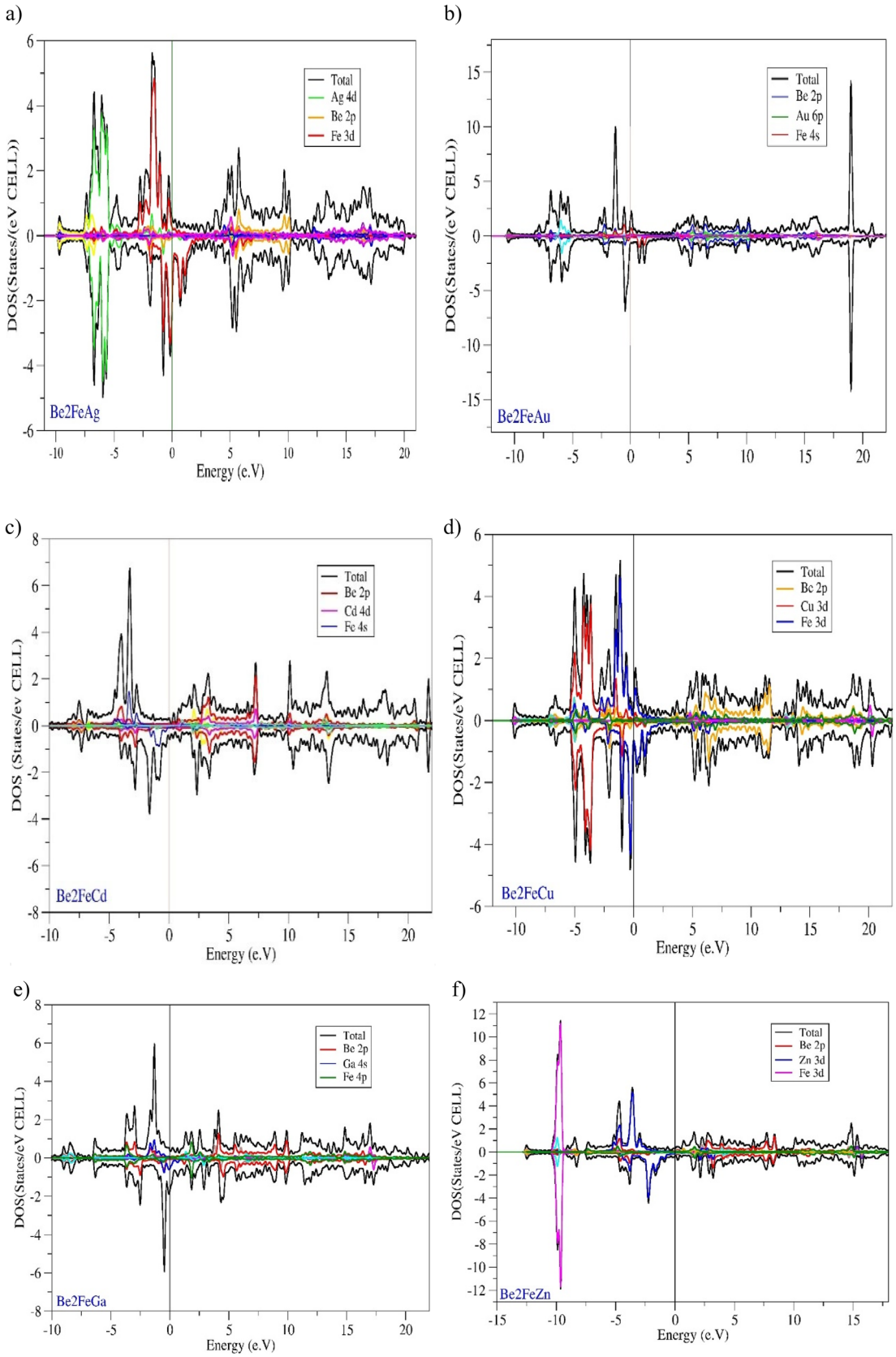

Fig. 7 DOS plots of the Be_2FeX (X = Ag, Au, Cd, Cu, Ga, Zn) alloys

Table 4 Total magnetization calculated for Be_2FeX (X = Ag, Au, Cd, Cu, Ga, Zn) Heusler alloys (μ_B)

Material	Be_2FeAg	Be_2FeAu	Be_2FeCd	Be_2FeCu	Be_2FeGa	Be_2FeZn
Total Magnetization	1.49	1.09	1.96	0.93	1.10	1.58

Author contributions

There is no experimental or theoretical study on the alloys mentioned in the article in the literature so far. And all calculations, tables, graphs and comments related to the study were carried out by Dr. Erol Albayrak.

Funding

Open access funding provided by the Scientific and Technological Research Council of Türkiye (TÜBİTAK). The authors declare that no funds, grants, or other support were received during the preparation of this manuscript.

Data availability

The raw/processed data required to reproduce these findings can be shared if requested. For questions regarding data, contact Erol Albayrak at erol.albayrak@ahievran.edu.tr.

Declarations

Competing interests The authors have no relevant financial or non-financial interests to disclose.

Ethical approval There was no situation that required ethics approval in this study.

References

1. T. Graf, F. Casper, J. Winterlik, C. Felser, J. Mater. Chem. C **7**, 2610 (2019)
2. E.D. Chernov, A.V. Lukoyanov, Magnetochemistry **9**, 185 (2023)
3. G.Y. Gao, K.L. Yao, Z.L. Liu, Sci. Technol. Adv. Mater. **21**, 647 (2020)
4. D.K. Yadav, S.R. Bhandari, G.C. Kaphle, M.P. Ghimire, R. Soc. Chem. **10**, 16179 (2020)
5. N.M. Fortunato, X. Li, S. Schönecker, R. Xie, A. Taubel, F. Scheibel, I. Opahle, O. Gutfleisch, H. Zhang, Chem. Mater. **36**, 6765 (2024)
6. J. Sjöberg, B. Sanyal, A. Delin, Phys. Rev. B **107**, 174402 (2023)
7. Z.S. Aliev et al., J. Alloy. Compd. **781**, 950 (2019)
8. X.-L. Qi, S.-C. Zhang, Rev. Mod. Phys. **83**, 1057 (2011)
9. A. Bansil, H. Lin, T. Das, Rev. Mod. Phys. **88**, 021004 (2016)
10. X. Liu, Y. Zhang, J. Wang, Z. Guo, Appl. Phys. Lett. **118**, 110601 (2020)
11. T. Xie, K. Li, Y. Wang, H. Zhang, Nano Energy **80**, 105490 (2021)
12. W. Huang, J. Chen, S. Lin, Adv. Func. Mater. **32**, 2108983 (2022)
13. Q. Zhang, Z. Luo, C. He, Phys. Rev. B **102**, 125403 (2020)
14. L. Jiang, W. Wei, Z. Sun, Mater. Today **56**, 110 (2023)
15. J. Xu, H. Wang, M. Li, Nat. Mater. **22**, 432 (2023)
16. M. Çanlı, E. Ilhan, N. Arıkan, Mater. Today Commun. **26**, 101855 (2021)
17. P. Giannozzi, O. Andreussi, T. Brumme, O. Bunau, M.B. Nardelli, M. Calandra et al., J. Phys.: Condens. Matter **29**, 465901 (2020)
18. T.A. Barnes, T. Kurth, P. Carrier, N. Wichmann, D. Prendergast, P.R. Kent, J. Deslippe, Comput. Phys. Commun. **214**, 52–58 (2017)

19. I. Carnimeo, F. Affinito, S. Baroni, O. Baseggio, L. Bellentani, R. Bertossa et al., J. Chem. Theory Comput. **19**(20), 6992–7006 (2023)
20. J.P. Perdew, K. Burke, M. Ernzerhof, Phys. Rev. Lett. **77**, 3865 (1996)
21. A.D. Corso, J. Phys.: Condens. Matter **28**, 075401 (2016)
22. O. Örnek et al., Russ. J. Phys. Chem. **95**, 2592 (2021)
23. S. Al-Qaisi et al., Results Phys. **7**, 709–714 (2017)
24. S. Alnujaim et al., Eur. Phys. J. B **95**(7), 114 (2022)
25. T. Seddik et al., Appl. Phys. A **106**, 645–653 (2012)
26. A. Bouhemadou et al., Phys. Lett. A **362**(5–6), 476–479 (2007)
27. S. Al, N. Arikan, A. Iyigör, Intermetallics **54**, 7 (2014)
28. P. Petit, Ann. de Chimie et de Phys. **10**, 395 (1819)